IOP Conf. Series: Earth and Environmental Science **71** (2017) 012002 doi:10.1088/1755-1315/71/1/012002

Tephra Fallout Hazard Assessment for VEI5 Plinian Eruption at Kuju Volcano, Japan, Using TEPHRA2

Tomohiro Tsuji[1], Michiharu Ikeda[1], Hiroshi Kishimoto[2], Koji Fujita[2], Naoki Nishizaka[3] and Kozo Onishi[3]

[1] Shikoku Research Institute Inc, 2109-8,Yashimanisi-machi, Takamatsu, 761-0192, Japan.
[2] Asia Air Survey Co. Ltd., Manpukuji, Asao-ku, Kawasaki, 215-0004, Japan.
[3] Shikoku Electric Power Co. Inc, 2-5, Marunouchi, Takamatsu, 760-8573, Japan.
Email: t-tsuji@ssken.co.jp

Abstract. Tephra fallout has a potential impact on engineered structures and systems at nuclear power plants. We provide the first report estimating potential accumulations of tephra fallout as big as VEI5 eruption from Kuju Volcano and calculated hazard curves at the Ikata Power Plant, using the TEPHRA2 computer program. We reconstructed the eruptive parameters of Kj-P1 tephra fallout deposit based on geological survey and literature review. A series of parameter studies were carried out to determine the best values of empirical parameters, such as diffusion coefficient and the fall time threshold. Based on such a reconstruction, we represent probabilistic analyses which assess the variation in meteorological condition, using wind profiles extracted from a 22 year long wind dataset. The obtained hazard curves and probability maps of tephra fallout associated to a Plinian eruption were used to discuss the exceeding probability at the site and the implications of such a severe eruption scenario.
Keywords: TEPHRA2; tephra fallout; simulation; Kuju Volcano; hazard assessment; probabilistic study.

1. Introduction

Nuclear power plants require extreme care to assure safety. The Volcanic Impact Assessment Guide for Nuclear Power Plants published by the Nuclear Regulation Authority [1] requires power plants to identify the volcanos that could affect them and take into consideration tephra fallout that could potentially occur due to eruptions during the operating life of the plants. In addition to literature reviews, geological surveys and volcanological surveys, the use of numerical simulation to estimate the volume of tephra fallout on power generation facilities has been increasing in recent years [2].

Although Shikoku has no active volcanoes, a large-scale eruption of a volcano located upwind on Kyushu could still affect various power generation facilities located in Shikoku via tephra fallout carried by the prevailing westerlies. Several active volcanoes are sitting on the volcanic front on the central to eastern regions of Kyushu Island (Figure 1). Kuju Volcano in particular among these active volcanoes has a history of major eruptions, and its eruption rates in the last 10,000 years have been high [3]; it is also recognized as one of the volcanoes that is most likely to affect the power plant in the future due to its location relative to the power plant [4]. The occurrence of tephra fallout from the major Kuju Volcano eruption 54,000 years ago has been confirmed in Shikoku [5, 6] (Figure 1b).

Although there is no record to indicate that the volcanic ejecta from Kuju Volcano eruption has fallen on the site of the Ikata Power Plant in the past, we must assume that tephra fallout could occur

depending on atmospheric conditions at the time of an eruption, particularly wind direction. The use of calculations to simulate advection, dispersal and deposition of tephra (e.g. TEPHRA2 [7], Fall3D [8, 9], HAZMAP [10], PUFF [11]) is an effective technique for forecasting the impact of tephra fallout from volcanic eruptions.

Several probabilistic assessment methods are available for forecasting the impact of tephra fallout during a future large-scale eruption [7, 12, 13]. A probabilistic assessment can be used to assess events that occur infrequently with a range of impacts that varies significantly depending on atmospheric conditions. If records of long-term meteorological observations are available, rare atmospheric conditions can be included in the assessment.

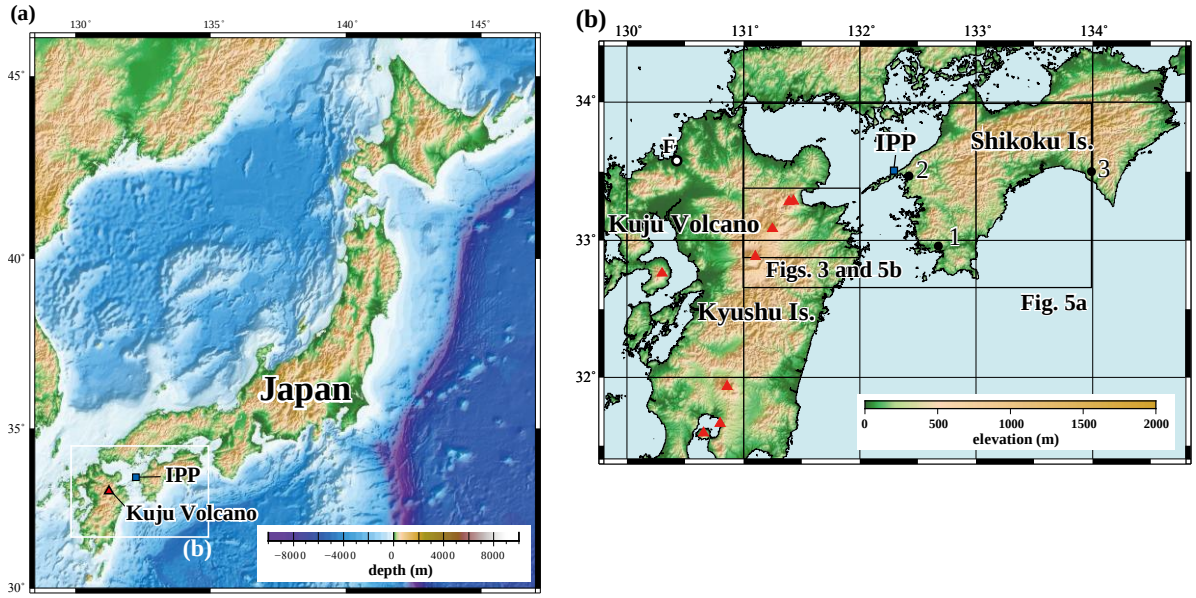

Figure 1. Maps of Japanese archipelago (a), and Kyushu and Shikoku Islands (b) showing localities of Kuju Volcano, Ikata Power Plant (IPP) and Fukuoka observation site (F). 1, 2 and 3 in (b) indicates localities of previous report of Kj-P1 tephras (Kumahara and Nagaoka [5], our unpublished data and Matsu'ura [6]). Red triangles represent active volcanoes. Area of Figs. 3, 5a and 5b are shown in (b).).

In order to probabilistically assess the volume of tephra fallout at the Ikata Power Plant in the event the Kuju Volcano erupts in a scale similar to the largest historical eruption that caused the Handa pyroclastic flow [3], we carried out a parameter study and probabilistic examination using a geological survey and tephra fallout simulation (TEPHRA2). In this paper, we present an outline of the air fall pumice from the Kuju eruption, followed by an estimation of the key eruption parameters (i.e., eruption volume, grain size and eruption column height) based on the results of our geological survey and existing literature. We then estimate the diffusion coefficient and fall time threshold by comparing the tephra fallout distribution between the results of our parameter study using TEPHRA2 and actual data. Based on the results, we develop an exceeding probability curve using wind data for 22 years [14] and a probability maps using wind data for a single year; the probabilistic assessment is discussed.

2. Outline of Kj-P1 fallout deposit

Kuju Volcano, which is located in central eastern Kyushu, has had three major VEI5-class [15] eruptions in the past [3]. The largest-scale eruption in recent time was the Handa pyroclastic eruption [3] about 54,000 years ago [16, 17]. A series of eruptions released, from the bottom layer, Kuju-D volcanic ash (Kj-D; 0.41 km^3), Handa pyroclastic flow (Kj-Hd; 5 km^3) and Kuju air fall pumice (Kj-P1) [18]. The volume of Kj-P1 is estimated to be 2.03 km^3 [19] or 6.2 km^3 [18].

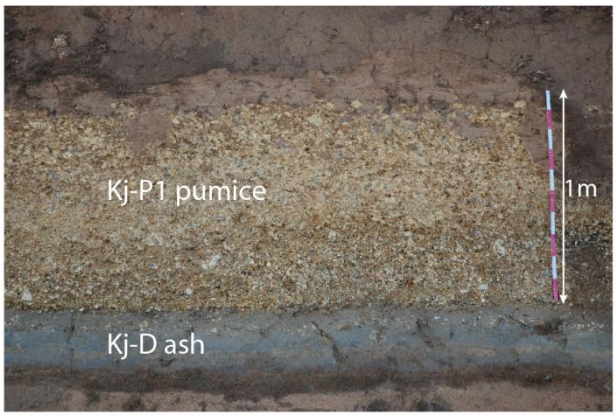

Figure 2. Occurrence of Kj-P1 air-fall pumice and Kj-D air-fall ash at about 19 km east from vent.

Kj-P1 consists mainly of dacitic pumice and lithic fragments. The pumice is rich in phenocryst, and contains heavy minerals such as hornblende, orthopyroxene and biotite. Near Kuju Volcano (within 25 km from the vent), it is accompanied by Kj-D at a lower level (Figure 2), presenting an unstratified, inversely graded structure. The axis of the distribution of layer thickness of Kj-P1 is primarily oriented eastward, with thin and wide distribution to the west (upwind) and north sides of the vent. The Kuju tephra is preserved in sediment in southwestern Shikoku about 150km away from the volcano [5], and its presence is confirmed as crypto-tephra in Yahatahama city 110 km away (unpublished data) as well as in the southeastern area of Shikoku about 280 km away [6] (Figure 1b).

Table 1. Input parameters of Kj-P1 tephra fallout deposit for analysis of TEPHRA2. TGSD; total grain size distribution.

Parameters	Case-1	Case-2	Case-3	References
Eruption Parameters				
Locality of the vent				
Easting		709900.1		[20]
Northing		3663051.9		
Elevation (m)		1971		
Erupted volume (km^3)		2.54		Field data
Plume height (km)		25		Field data, [21]
TGSD				
Md phi		1.5		Field data, [22]
Sigma phi		3.0		
Grain parameters				
Diffusion coefficient (m^2/s)	200-10000	10000	10000	comparison with TEPHRA2 and field data
Fall time threshold (s)	200 -3000	1000	1000	
Dencity (kg/m^3)				
Pumice		1000		[7]
Lithic		2600		
Wind parameters				
Wind speed	Feb. 2010	1988-2010	2010	[14]
Wind direction	Feb. 2010 +8 degree	1988-2010	2010	

3. Methodology

We used TEPHRA2, which has a proven track record in tephra fallout simulation, for the analysis in this study. TEPHRA2 is a simulation program based on an advective diffusion model [7]. TEPHRA2 can calculate the distribution of deposits by providing appropriate initial parameters [23]. It is suitable

for parameter studies and probabilistic assessments as it can readily and rapidly perform the calculations. The analytical program is downloadable from the site at the University of South Florida (http://www.cas.usf.edu/~cconnor/vg@usf/tephra.html). Four types of parameters are required for calculation, namely, eruption, atmospheric, grain and grid (Table 1). For the atmospheric parameters, we used the Yearbook of Aerological Observation [14] (Table 1). For the grid parameters, we developed a 2-km grid mesh using digital maps available from the Geospatial Information Authority of Japan (50-m DEM) and the National Institute of Advanced Industrial Science and Technology (1-km DEM). Calculations with TEPHRA2 produce tephra fallout per unit area (kg/m^2) and its grain composition. In our study, we express this as layer thickness (cm) per unit area, assuming that the density of the pyroclastic fall is 1000 kg/m^3.

4. Reconstruction of Eruptive Parameters of Kj-P1 Fallout Deposit

The important eruption parameters that determine the characteristics of an eruption consist mainly of coordinates of the vent, eruption volume, grain size, and eruption column height. For the coordinates of the vent, we referred to the coordinates of Nakadake given in the catalogue published by the Japan Meteorological Agency [20] (Table 1). As the eruption volume and grain size have a significant impact on the results, they should be estimated accurately by a geological survey. However, the grain size and eruption column height of Kj-P1 have not been examined in the past. In this study, therefore, we carried out a geological survey with respect to Kj-P1 and estimated the eruption volume, grain size and eruption column height of the eruption.

4.1. Eruptive Volume

In this study, we successfully reconfirmed the outcrops that had been identified by Nagaoka & Okuno [18], and expanded the dataset by adding new exposed outcrops (Figure 3). We set the survey points more densely along the principal axis of distribution that was important for examination of layer thickness and grain size (e.g. one collection point per 2 km^2) in order to collect a larger volume of data. Based on the collected data, we then examined the eruption volume by methods used for calculation of eruption volume including the contour method, the Hayakawa Method [24] and the Weibull Method [25].

4.1.1. Conter Method

We added reports for three areas in Shikoku to the results of our survey in Kyushu, and drew an isopach map by partitioning layer thickness (cm) into bins of >200, 200–100, 100–50, 50–25, 25–10, 10–5, 5–2, and 2–1 cm. We calculated the eruption volume to be 1.95 km^3 by totaling the values obtained by multiplying each of the layer thicknesses by its area. Note that we did not estimate the volume of the layer less than 1-cm thick with this method.

4.1.2. Weibull Method

The Weibull Method approximates the relationship between layer thickness T (cm) and area of isopach A (km^2; $A=x^2$) by the following formula:

$$T = \theta(x/\lambda)^{k-2}e^{\wedge}(x/\lambda)^{k}$$

Where λ is the attenuation length of deposit layer thickness (km), and k and θ the scale of layer thickness (cm; $\theta = eT(\lambda)$). The value of e is 2.718 (Euler/Napier constant) and k is a dimensionless shape parameter. According to this formula, the eruption volume of tephra V (km^3) is calculated by the following formula:

$$V = \int TdA = 2\theta\lambda^2/k$$

where λ, θ and k are determined by the method of least squares with the measured values. The Weibull Method requires the use of a specified range of layer thickness data. The eruption volume was

estimated to be 1.85 km^3 using 4 isopachs of the layer thicknesses from 500 cm to 50 cm, 3.26 km^3 using 5 isopachs including layer thicknesses to 25 cm, and 2.25 km^3 using 6 isopachs including layer thicknesses to 10 cm.

4.1.3. Hayakawa Method

The Hayakawa Method expresses the eruption volume V (km^3), layer thickness T (cm) and area of isopach A (km^2) by the following formula:

$$V = 12.2TA$$

The Hayakawa Method requires the use of a specified layer thickness. In order to increase the accuracy of the eruption volume, we used the layer thickness of 100 cm, which had the highest data density and closed contour lines. Using the layer thickness of 100 cm, the eruption volume was estimated to be 2.54 km^3.

4.1.4. Eruptive Volume for Analysis

Using the above three techniques, we estimated the eruption volume to be between 1.95 and 3.26 km^3. We then examined the eruption volume to be used in our analysis by comparing these results. As the estimate by the contour method does not include areas with less than 1cm-thick layer, the actual eruption volume is presumed to be more than 1.96 km^3. The Weibull Method produced different results depending on the range used although the variations are not great. The average of the three estimates produced by the Weibull Method was 2.45 km^3. The eruption volume of 2.54 km^3 as calculated by the Hayakawa Method using the layer thickness of 100 cm is comparable to the average of three values calculated by the Weibull Method. It was also consistent with the result of the contour method that indicated the volume to be more than 1.95 km^3. Based on the results of the above examination, we set the eruption volume to be used in our analysis to be 2.54 km^3 (Table 1). This value is close to 2.03 km^3 estimated by Suto et al. [19] but considerably smaller than 6.2 km^3 set by Nagaoka and Okuno [18]. The reason for this difference may be due to the estimates made by Nagaoka and Okuno [18] for distant sites, particularly Shikoku and eastward, being too large. In a case, such as Kj-P1, in which the layer thickness data at distant sites is scarce, we believe that the use of techniques that allow estimation based on data for data-rich areas improves the reliability of eruption volume estimates.

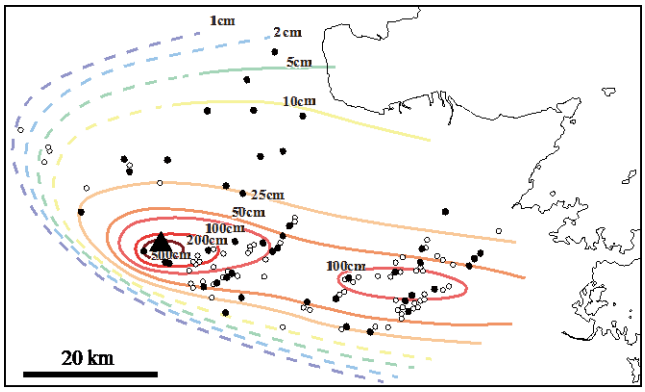

Figure 3. Isopach map and localities of outcrops for Kj-P1 deposit. Black and open circles are localities of our unpublished data and data compiled data from [18]. Black triangle indicates the crater of Kuju Volcano.

4.2. Total grain-size distribution

It is difficult to accurately estimate the grain size in the whole tephra (i.e., total grain size distribution; TGSD) from old and weathered pyroclastic fallout, such as Kj-P1, due to the conditions

of outcrops and the effects of weathering [2]. Accordingly, we collected samples from outcrops that were relatively unweathered and therefore measurable, analyzed their grain sizes using a sieve method and a laser diffraction/scattering grain size distribution measuring apparatus (Nikkiso Microtrac Ver. 10.4.2) in order to obtain the median grain size (Mdφ) ($\varphi = -\log_2 D$, D = diameter (mm)) as well as the sortedness (σφ) [26]. We then estimated the median grain size and dispersal of Kj-P1 by comparing this value against the data for tephra for which TGSD had been examined in detail. As a product of an eruption that had the eruption volume, magma composition, quantity of crystals, layer thickness distribution and grain size that were similar to Kj-P1, we selected Ta-b pumice fallout from Tarumae Volcano [22]. Ta-b is a crystal-rich andesitic pumice fallout having a scale of eruption and layer thickness distribution that are similar to Kj-P1. According to Suzuki et al. [22], the eruption volume of Ta-b was 1.96 km^3 with average grain size Mdφ of –0.32φ and sortedness of 3.2φ [22].

4.2.1. Median grain-size

Figure 4 presents the grain size data collected from the area located between about 5 km to 50 km from the vent along the principal axis of the Kj-P1 distribution. The median grain size of Kj-P1 (Mdφ) at 10 km from the vent was about –2φ and at 40 km 0φ, indicating that it became finer rapidly with increasing distance from the vent (Figure 4). This is because coarse-grained particles fall out first as the volcanic eruption column travels through the atmosphere. A logarithmic curve well approximates the changes in the grain size of Kj-P1 with distance (Figure 4).

Ta-b contains a number of fall units; one of these, Ta-b_8, is the most coarse-grained fall unit and its TGSD is well understood [22]. The plot of the median grain size of Ta-b_8 distributed downwind from the vent along the principal axis of distribution is presented in Figure 4. Changes in the median grain size of Ta-b_8 with distance from the vent can be approximated by a logarithmic curve in the same way as for Kj-P1 (Figure 4).

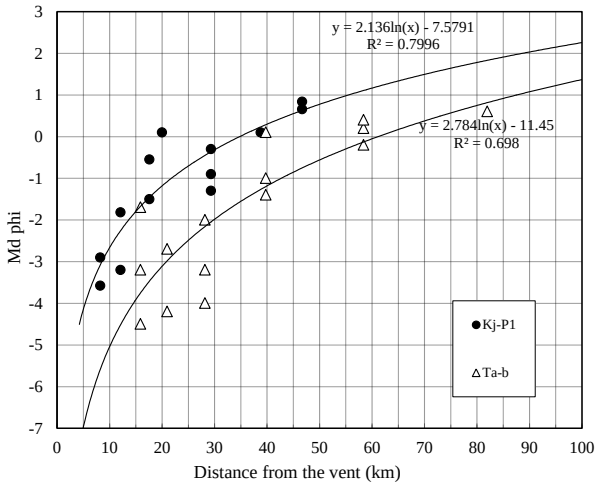

Figure 4. Plots of average grain size Mdφ of Kj-P1 (black circle) and Ta-b (white triangle) [22] distributed downwind along the axes of distribution from vent.

Next, we estimated the grain size distribution for the entire Kj-P1 by reading the differences in grain diameters of Ta-b_8 and Kj-P1from Figure 4. Generally, the TGSD of the tephra is significantly affected by the grain size of the deposit near the vent [27]. This stems from the fact that a majority of tephra is deposited in the vicinity of the vent. Furthermore, Suzuki et al. [22] pointed out that the layer thickness of Ta-b_8 became exponentially thinner with distance from the vent. Accordingly, we identified the median grain size at distances of 5, 10, 20, 40, and 80 km from the vent so that the degree of the effect on grain size farther away from the vent was exponentially smaller. Differences at each distance were, for example, 2.85φ at 5 km, 1.95φ at 20 km, 1.05φ at 80 km (Figure 4). In addition, Suzuki et al. [22] estimated the tephra fallout that was deposited 100 km or farther away from the vent

to be approximately 20% of the total eruption volume. In order to consider this, we extrapolated the approximate curves in Fig. 4 to 160 km from the vent, and found that the difference was approximately 0.95φ. We adopted this value as representative of the differences in the grain size in the areas 100 km or farther away from the vent. The above examination indicates that the grain size of Kj-P1 was 0.95 to 2.85φ smaller than that of Ta-b at the same distance from the vent. In addition, we averaged the values at these distances and estimated that the grain size of Kj-P1 was 1.77φ smaller than that of Ta-b_8. Since the median grain size of the entire Ta-b is –0.32φ [22], we estimated Mdφ for Kj-P1 to be about 1.45φ. As a result, we used the value of 1.5φ for the median grain size in our analysis (Table 1). Since the typical grain size distribution in tephra generally has a median grain size of –1 to 4φ or smaller [2], the result of our examination is consistent with this range.

4.2.2. Sortness (Standard Deviation)

The approximate curves of Kj-P1 and Ta-b_8 presented in Figure 4 show similar gradients, which indicates that both are similar to each other in terms of the trends for change in grain diameter with distance and the width of the grain diameter distribution. In this study, we used this similarity in determining the sortedness, an indicator for the width of grain size distribution [26], and set the sortedness of Kj-P1 to be 3φ, which was similar to 3.2φ for Ta-b (Table 1). The result of our examination is consistent with the sortedness of tephra from Plinian eruptions being 2 to 3φ [2], as is generally believed.

4.2.3. Column height

With respect to eruption column height for which there are no observation records, a model that reconstructs the data from grain size has been proposed by Carey and Sparks [21]. In this study, we measured the downwind range and the crosswind range [21] for the grain size of the tephra deposit according to their eruption column model. We measured long and short axes of five grains taken from the largest grains of pumice and lithic fragments observed in outcrops, and determined the largest grain diameter by averaging their values. The downwind ranges of pumice with the largest grain diameters of 4 and 2 cm were 23.0 and 51.3 km and the crosswind ranges for the pumice grains were 8.7 and 12.8 km, respectively. The downwind ranges of lithic fragments with diameters of 3.2 and 1.6 cm were 21 and 39 km and the crosswind ranges of the lithic fragments were 5.1 and 9 km, respectively. By comparing these results with the model map by Carey and Sparks [21], the eruption column height of Kj-P1 was estimated to be 22 to 28 km. The eruption column heights estimated by varying the grain size were relatively consistent. Accordingly, we selected a column height of 25 ± 3 km for our analysis (Table 1). This estimate is consistent with the eruption column height of a VEI5-class eruption, which is the scale of the Kj-P1 eruption, being 20 to 35 km, as stated by Newhall and Self [15]. The effect of changes in the eruption column heights on thickness distribution of the tephra deposit was examined by Tsuji et al. [4] using values in a range of 20, 25 and 30 km, and was confirmed not to have a major effect on the results.

5. Reconstruction of Grain Parameters

In order to set the grain parameters, we needed data for densities of pumice and lithic fragments, diffusion coefficient, fall time threshold and volcanic eruption column model. For the densities of pumice and lithic fragments, we referred to Bonadonna et al. [7] (Table 1). In the following sections, we examine reasonable values for the diffusion coefficient and fall time threshold by comparing the thickness distribution of the tephra deposit layers that we observed in our field study against the results of our parameter study using TEPHRA2.

5.1. Wind Selection

In order to determine the values of the diffusion coefficient and the fall time threshold for our analytical model, we deterministically selected wind profiles. Tsuji et al. [4] examined the effects of changes in the direction and velocity of wind by month based on the normal values by month, which

represented the average of the wind directions and velocity data collected at various observation sites at altitudes between ground level and 30 km [14]. According to the results, tephra fallout is carried northeastward from the vent and distributed in a slightly wide area in summer (July–September) when the wind is weak. In contrast, the tephra fallout is carried eastward in winter (December–February) in a narrow distribution pattern due to strong westerlies [4]. As the analytical results for the winter are comparable to the actual layer thickness distribution of Kj-P1, we used winter wind (February) as the comparative wind profile. In order to reconcile the direction of primary axis of the deposit distribution of the analytical results and the field data, however, we adjusted the direction of the normal February wind profile northward by 8 degrees.

5.2. Diffusion coefficient and fall time threshold

We carried out an analysis by varying the diffusion coefficient between 200 and 10,000 m^2/s and the fall time threshold between 200 and 3000 s in order to find the diffusion coefficient and fall time threshold at which the computed layer thickness (the "computed data") and the observed layer thickness (the "observed data") matched the best. The diffusion coefficient of 10,000 m^2/s and the fall time threshold of 1000 s matched best with the results of our survey (Figs. 5 and 6). Figure 6 presents a comparison of the computed and observed data for diffusion coefficient of 10,000 m^2/s and fall time threshold of 1000 s. The results show a positive correlation between the computed and observed data (Figure 6). The layer thickness was thinner in the range of 5–25 cm for the computed data than the observed data whereas the layers were slightly thicker in the range of 40–130 cm for the computed data (Figure 6). Overall, the deposit layers were slightly thicker in the computed data than in the observed data (Figure 6).

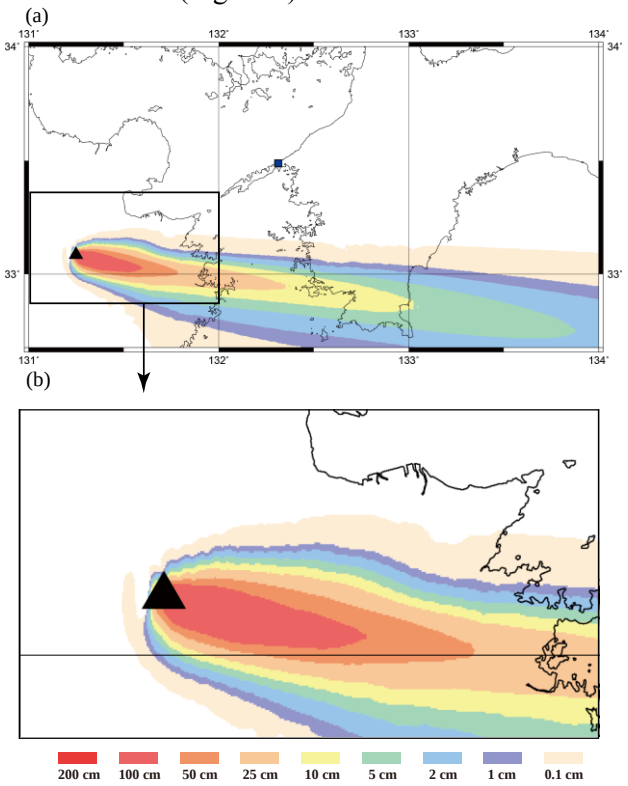

Figure 5. Calculated result with the value of case-1 (diffusion coefficient, 10000; fall time threshold, 1000; Table 1).

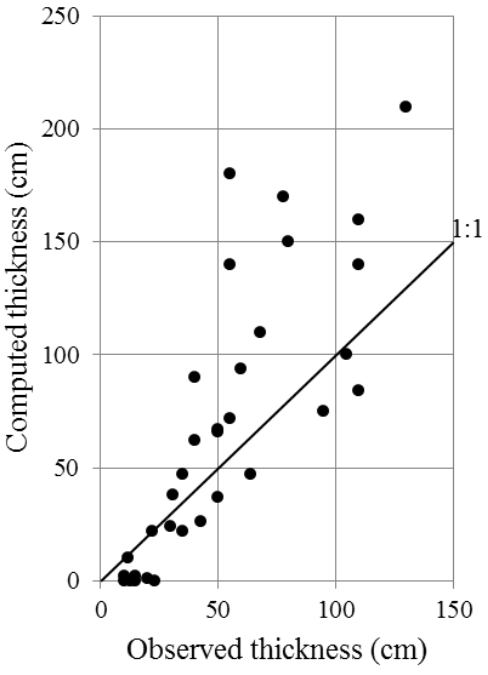

Figure 6. Comparison between observed data and data computed with the same value of Figure 5.

In our parameter study, we could not satisfactorily reproduce the tephra fallout distribution spread thinly on the west (upwind) and north sides of the vent (Figure 3 and 5b). We need to review the

possibilities that the eruption rate or the wind direction/velocity changes during the eruption or that the wind direction varies by altitude.

6. Result and Discussion

6.1. Hazard Curves

Based on the eruption and grain parameters (Table 1) obtained by the work described above, we developed a hazard curve for the Ikata Power Plant using daily wind profiles for the 22-year period from 1988 to 2010 compiled by the Japan Meteorological Agency [14] (Case-2 of Table 1). The wind data represent the wind profiles at 9am at the Fukuoka Observation Station for 7976 days between March 1, 1982 and December 31, 2010 (Table 1). Figure 7 presents the exceeding probability curve at Ikata Power Plant. Generally, volcanic ash fall causes poor visibility and difficulty in uphill driving for automobiles at an accumulation of 1 cm, and may pose risk for collapse of structurally weak houses at 10 cm [28, 29]. The results of our present analysis indicated that the probability of ash fall of 10 cm or more at Ikata Power Plant was 4.44% and 5 cm 12.74%. The probability of exceedance with respect to thickness of Kuju Volcano origin ash fall at the Ikata Power Plant is obtained by multiplying each of these values by the probability of eruption.

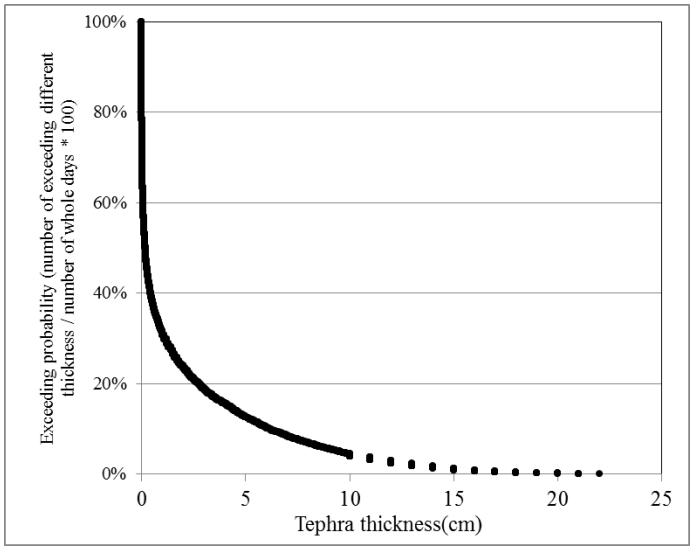

Figure 7. Hazard curve shows the conditional probability of exceeding different thickness of tephra at Ikata Power Plant, given a VEI5 volcanic eruption. The curve was generated from TEPHRA2 output, based on the simulations for 7976 days from March 1, 1982 to December 31, 2010 with the value of case-2 (Table 1).

6.2. Probability Maps

Based on the eruption and grain parameters obtained by the above work (Table 1), we developed a distribution map of the probability of exceedance for ash fall from an eruption of Kj-P1 scale (Figure 8). This map shows that the probability of a 1 cm-thick ash fall during an eruption of Kj-P1 scale is higher than 80% in western area of Usuki city and 40–60% between Yahatahama and Sukumo area in southwestern Shikoku. The probability falls rapidly in the areas further south and north with a probability of about 30% at the Ikata Power Plant site. For 5-cm thick ash fall, the probability is higher than 60% in western area of Usuki city and 10–30% in southwestern Shikoku. As the above results indicate, the probability of thick ash fall from the Kuju Volcano eruption is higher on the east side of the crator. This is a result of the strong influence of the jet stream (westerlies) flow at around an altitude of 10 km.

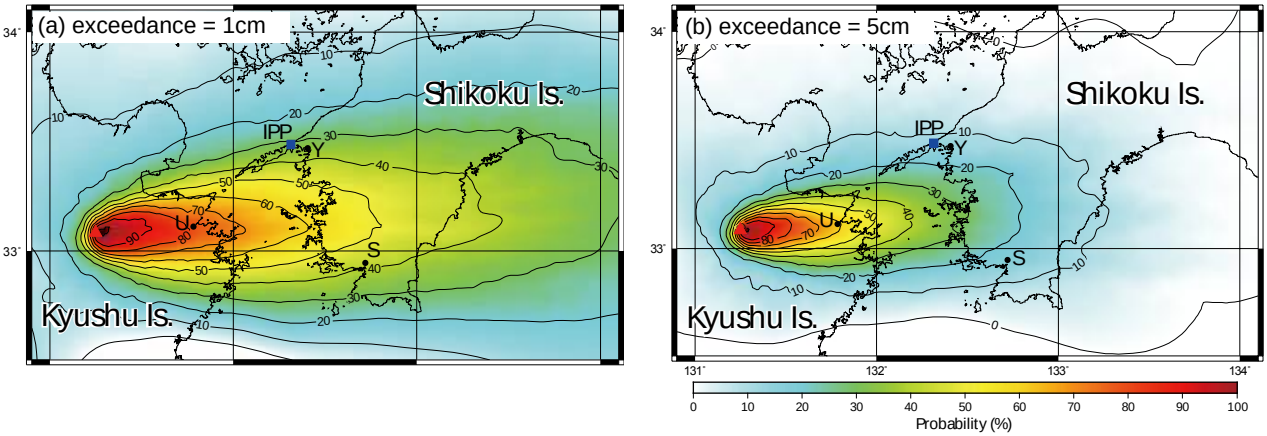

Figure 8. The maps contour the probabilities of tephra accumulations exceeding 1 cm (a) and 5 cm (b), given a VEI5 plinian scenario. The maps were generated from the TEPHRA2 output, based on the simulations for 365 days for 2010 with the value of case-3 (Table 1). IPP: Ikata Power Plant, S: Sukumo city, Y: Yahatahama city, U: Usuki city.

7. Conclusions

In this study, we carried out a geological survey and literature review and estimated the eruption parameters (eruptive volume, TGSD and column height) for a Plinian eruption (Kj-P1) under a VEI5 scenario, which are the most basic as well as the most important data for the assessment of volcanic eruption risks. Furthermore, we estimated the grain parameters (diffution coefficient and fall time threshold) by comparing the tephra fallout distribution between the results of our parameter study using TEPHRA2 and actual data. On the basis of such a reconstruction, we analysed TEPHRA2 using 22-year long record of wind profiles and obtained the results indicating that the probability of ash fall of 10 cm or more at Ikata Power Plant was 4.44% and 5 cm 12.74%. This study also estimate the probability of the range and volume of ash fall during a future large-scale eruption of Kuju Volcano. These findings should contribute to the development of hazard maps not only for Ikata Power Plant but also for regions located downwind from the vent.

8. Acknowledgements

The authors would like to sincerely thank D. Miura, K. Toshida, S. Takeuchi, Y. Hattori, S. Uesawa for their insightful discussions on eruption process, simulation of Kj-P1 eruption and volume calcuration techniques. H. Inakura and K. Mannen provided valuable information about TEPHRA2 technique. M. Okuno provided helpful comments on eruptive process. T. Tsuji also thanks T. Ouchi for correcting English, F. Suzuki for assistance in grain size analysis, TEPHRA2 simulation operation and making figures, T. Yanagihara and S. Yamamoto for their kindful support on grain size analysis. Some of the figures in this paper were made using the Generic Mapping Tools [30].

9. References

[1] Nuclear Regulation Authority, 2013. Volcanic Impact Assessment Guide for Nuclear Power Plants. p. 26 (Japanese).
[2] Volentic, A. C. M., Connor, C. B., Connor, L. J. And Bonadonna, C., 2009. Aspects of volcanic hazard assessment for the Bataan nuclear power plant, Luzon Peninsula, Philippines. In: Connor, C. B. et al. (eds.) Volcanic and Tectonic Hazard Assessment for Nuclear Facilities. Cambridge University Press, 229-256.
[3] Kawanabe, Y., Hoshizumi, H., Ito, J. and Yamazaki, S., 2015. Geological map of Kuju Volcano. 1: 25,000 in scale, National Institute of Advanced Industrial Science and Technology, Geological map of volcanoes, 19 (Japanese with English abstract).

[4] Tsuji, T., Ikeda, M., Kato, S., Nishizaka, N. and Onishi, K., 2015. Simulation analysis for air-fall ash influences on Shikoku Island. Research Report of Shikoku Electoric Power Co. and Shikku Research Institute, 103, 9-21 (Japanese with English Abstract).
[5] Kumahara, Y. and Nagaoka, S., 2002. Identification of the Kuju-Daiichi Tephra Layer, and the Age of the Late Pleistocene Fluvial Terrace along the Matsuda River in Southwestern Shikoku, Japan. The Quaternary Research, 41, 213-219 (Japanese with English abstract).
[6] Matsu'ura, T., 2015. Late Quaternary uplift rate inferred from marine terraces,Muroto Peninsula, southwest Japan: Forearc deformation in an oblique subduction zone. Geomorphology, 234, 133-150.
[7] Bonadonna, C., Connor, C. B., Houghton, B. F., Connor, L., Byrne, M., Laing, A. and Hincks, T. K., 2005. Probabilistic modeling of tephra dispersal: Hazard assessment of a multiphase rhyolitic eruption at Tarawera, New Zealand. Journal of Geophysical Research, 110, B03203, doi:10.1029/2003JB002896.
[8] Costa, A., Macedonio, G. and Folch, A., 2006. A three-dimensional Eulerian model for transport and deposition of volcanic ashes. Earth Planet Sci. Lett., 241, 634–647.
[9] Folch, A., Costa, A. and Macedonio, G., 2009. FALL3D: A computational model for transport and deposition of volcanic ash, Comput. Geosci., 6, 1334–1342.
[10] Macedonio, G., Costa, A. and Longo, A., 2005. A computer model for volcanic ash fallout and assessment of subsequent hazard. Comput. Geosci. 31, 837–845.
[11] Searcy, C., K. Dean, and W. Stringer (1998), PUFF: A high-resolution volcanic ash tracking model, J. Volcanol. Geotherm. Res., 80, 1–16.
[12] Bonasia, R., Capra, L., Costa, A., Macedonio, G. and Saucedo, R., 2011. Tephra fallout hazard assessment for a Plinian eruption scenario at Volcán de Colima (Mexico). Journal of Volcanology and Geothermal Research 203, 12–22.
[13] Bonasia R., Costa, A, Folch, A., Macedonio, G. and Capra, L., 2012. Numerical simulation of tephra transport and deposition of the 1982 El Chichón eruption and implications for hazard assessment., Journal of Volcanology and Geothermal Research, 231-232, 39-49.
[14] Japan Meteorological Agency, 2012.
[15] Newhall, C. G. and Self, S., 1982. The volcanic explosivity index (VEI) an estimate of explosive magnitude for historical volcanism. Journal of Geophysical Research, 87(C2), 1231-1238.
[16] Okuno, M., Nagaoka, S. and Kobayashi, T., 2012. Studies on Eruptive History of Kuju Volcano: A Review. Summaries of Researches Using AMS at Nagoya University, XXIII, 164-170.
[17] Nagaoka, S. and Okuno, M., 2015. Eruptive History of Kuju Volcanic Group, SW Japan. Transactions, Japanese Geomorphological Union, 36, 141-158.
[18] Nagaoka, S. and Okuno, M., 2014. Tephra-staratigraphy of Kuju Volcano in southwest Japan. Monthly Earth, 36, 281-296 (Japanese with English abstract).
[19] Suto, S., Inomata, T., Sasaki, H. and Mukoyama, S., 2007. Data base of the volcanic ash fall distribution map of Japan. Bulletin of Geological Survey of Japan, 58, 261-321 (Japanese with English Abstract).
[20] Japan Meteorological Agency, 2013. National catalogue of the active volcanoes in Japan (The fourth edition).
[21] Carey, S. and Sparks, R. S. J., 1986. Quantitative models of the fallout and dispersal of tephra from volcanic eruption columns. Bull. Volcanol. 48, 109–125.
[22] Suzuki, T., Katsui, Y. and Nakamura, T., 1973. Size Distribution of the Tarumai Ta−b Pumice−fall Deposit. Volcanology, 18, 47-63 (Japanese with English Abstract).
[23] Mannen, K., 2013. Theoretical background and recent progress of the pyroclastic fall simulation code Tephra2 : essence for application in Quaternary research. The Quaternary Research, 52, 173-187 (Japanese with English abstract).
[24] Hayakawa, Y., 1985. Pyroclastic Geology of Towada Volcano. Bulletin of the Earthquake Research Institute, University of Tokyo, 60, 507-592.
[25] Bonadonna, C. and Costa, A., 2012. Estimating the volume of tephra deposits: a new simple

strategy, Geology, 40, 415-418.
[26] Inman, D. L., 1952. Measures for describing the size distribution of sediments. J. Sediment. Petrol., 22, 125-145.
[27] Bonadonna, C., and Houghton, B.F., 2005, Total grain-size distribution and volume of tephra-fall deposits. Bull. Volcanol., 67, 441-456.
[28] Barnard, S., 2003. Potential effects of any future 1886-type eruption from Tarawera volcano on the Bay of Plenty region. Unpublished MSc thesis, University of Canterbury, Christchurch.
[29] Tauranga-WBOP Emergency Management, 2002. Civil Defence Plan 2002. Emergency management Office, Western Bay of Plenty District Council, Tauranga.
[30] Wessel, P. and Smith, W.H.F., 1995, New Version of the Generic Mapping Tools released. EOS, 76, 329.